bioRxiv preprint doi: https://doi.org/10.1101/661975; this version posted June 6, 2019. The copyright holder for this preprint (which was not certified by peer review) is the author/funder, who has granted bioRxiv a license to display the preprint in perpetuity. It is made available under aCC-BY-ND 4.0 International license.

DECODING THE MECHANOCHEMISTRY OF NEURITE PLASTICITY

Katherine M. Pearce[1,*], Miriam Bell[2,*], Will H. Linthicum[3], Qi Wen[3], Jagan Srinivasan[4], Padmini Rangamani[2,$] , and Suzanne Scarlata[1,$]

Affiliations:
1: Department of Chemistry and Biochemistry, Worcester Polytechnic Institute, Worcester, Massachusetts 01609
3: Department of Biomedical Engineering, Worcester Polytechnic Institute, Worcester, Massachusetts 01609
4: Department of Biology and Biotechnology, Worcester Polytechnic Institute, Worcester, Massachusetts 01609
2: Mechanical and Aerospace Engineering Department, University of California San Diego, La Jolla, CA 92093

* -- both these authors contributed equally to this study
$ -- corresponding authors: sfscarlata@wpi.edu, prangamani@ucsd.edu

Lead author – S. Scarlata, sfscarlata@wpi.edu

bioRxiv preprint doi: https://doi.org/10.1101/661975; this version posted June 6, 2019. The copyright holder for this preprint (which was not certified by peer review) is the author/funder, who has granted bioRxiv a license to display the preprint in perpetuity. It is made available under aCC-BY-ND 4.0 International license.

Abstract:

Normal calcium responses to hormones and neurotransmitters are critical for neuronal health. Calcium responses are carried out by the Gαq/phospholipase Cβ (PLCβ)/ phosphatidylinositol 4,5 bisphosphate (PI(4,5)P_2) signaling pathway. Here, we show that Gαq stimulation results in the retraction of neurites in PC12 cells and rupture of neuronal synapses. To understand the underlying cause, we dissected the behavior of individual components of the Gαq/PLCβ /PI(4,5)P_2 pathway during retraction, and correlated these to the retraction of the membrane and cytoskeletal elements impacted by calcium signaling. We developed a mathematical model that combines biochemical signaling with membrane tension and cytoskeletal mechanics, to show how signaling events are coupled to retraction velocity, membrane tension and actin dynamics. The coupling between calcium and neurite retraction is shown to be operative in the *C. elegans* nervous system. This study uncovers a novel mechanochemical connection between the Gαq/PLCβ /PI(4,5)P_2 pathway that couples calcium responses with neural plasticity.

Keywords: neurodegeneration, calcium signaling, modeling, neurite retraction, G protein signaling, *C. elegans*

INTRODUCTION:

Throughout the course of an organism's life, different neuronal connections break and reform to generate new electrical patterns that allow for optimal function during development and through adulthood. This plasticity of neuronal connections allows the rewiring of circuitry necessary for memory and learning (e.g.(Takeuchi et al.) (Stuchlik, 2014) (Licht et al., 2011)). Understanding the factors that permit appropriate and efficient rewiring is essential for understanding both developmental and neurodegenerative diseases.

Calcium is a key mediator of neuronal functions such as axonal growth, neurite protrusion, and spinogenesis (Brini et al., 2014; Clapham, 2007). The role of calcium in neurite growth and protrusions associated with development has been studied in different contexts (e.g (Mattson, 2007)). This outgrowth process is stimulated by neurotrophic factors that carefully regulate the spatiotemporal aspects of intracellular calcium. Neurite growth can also be triggered by stress, pharmacological agents, or starvation (Gilbert and Man, 2017; McKay et al., 1999). These factors may occur during disease states and contribute to inappropriate neurite growth, which can result in an increased number of smaller and non-productive neurites, as seen in autism (Gilbert and Man, 2017).

Neurodegenerative diseases are associated with the disruption of normal calcium signaling. Specifically, diseases such as autism and amyotrophic lateral sclerosis (ALS) have been linked to over-excitation of neurons or excitotoxicity caused by abnormal calcium homeostasis (King et al., 2016). Understanding the link between dysfunction of cellular calcium, particularly prolonged signaling, and neuronal function is critical to understand the mechanisms that underlie diseases typified by inappropriate neuronal excitation. While previous research has focused on the short-term effects of elevated cellular calcium after stimulation and its effects on neurite growth (Rosenberg and Spitzer, 2011), little is known about the effect of extended elevated calcium on these same neurites over time, i.e. cases that mimic an extended overstimulated state. In this study,

bioRxiv preprint doi: https://doi.org/10.1101/661975; this version posted June 6, 2019. The copyright holder for this preprint (which was not certified by peer review) is the author/funder, who has granted bioRxiv a license to display the preprint in perpetuity. It is made available under aCC-BY-ND 4.0 International license.

we investigate the effects of prolonged stimulation of Gαq/PLCβ/PIP_2 /calcium signaling pathway in a model neuronal cell line, PC12, and in the neuronal network in a small organism, *Caenorhabditis elegans*.

Calcium signals in neurites can be generated by several mechanisms. In synapses, postsynaptic cells receive an influx of calcium directly through the opening of transmembrane channels in response to neurotransmitter release (Voglis and Tavernarakis, 2006). Neurotransmitters, such as acetylcholine, activate G protein coupled receptors (GPCRs) on the plasma membrane to generate the release of calcium from intracellular stores (McKay et al., 1999). Furthermore, neurotropic factors activate receptor tyrosine kinases to increase intracellular calcium through another phospholipase C family, PLCγ. Downstream from these events are the opening of calcium-activated calcium channels on the endoplasmic reticulum (ER) membrane. Many of these channels are thought to respond to the increase in cytosolic calcium and to changes to the physical properties of the plasma membrane. These increases in cellular calcium regulate specific transcription factors and post-transcriptional processes that lead to appropriate downstream responses (West et al., 2001).

In this study, we show that neurites will completely retract to the soma by extended stimulation of the GPCR/Gαq/PLCβ pathway. This pathway mediates signals from many hormones and neurotransmitters such as acetylcholine, dopamine, histamine, and melatonin (Kadamur and Ross, 2013). Signaling begins with ligand binding to its specific G protein coupled receptor to activate the Gαq family of G proteins by exchange of GTP for GDP. The GTP-bound Gαq subunits then actives phospholipase Cβ (PLCβ). PLCβ catalyzes the hydrolysis of phosphatidylinositol 4,5-biphosphate (PIP_2) to inositol 1,4,5-triphosphate (IP_3) and diacylglycerol (DAG). IP_3 binds to receptors on the endoplasmic reticulum allowing the release of calcium from intracellular stores into the cytoplasm. The elevated calcium can then change the activity of a variety of intracellular proteins to generate a specific cell response.

Incorporated in this pathway are a number of positive and negative feedback loops. The initial calcium release generated by PLCβ in turn stimulates the highly active PLCδ that synergizes the calcium response (Guo et al., 2005). Increased calcium also opens calcium-induced calcium channels, further strengthening calcium responses (Lohmann and Wong, 2005). Negative feedback comes from the internalization of ligand-bound receptors into endosomes over a few minutes that typically return unbound receptors to the plasma membrane over a period of 20-30 min (Freedman and Lefkowitz, 1996). Additionally, Gαq has a GTPase activity that returns it to the basal state and this activity is stimulated by the GTPase activating (GAP) activity of PLCβ (Berstein et al., 1992), along with RGS proteins that quickly turn-off the signal (Dohlman and Thorner, 1997). It is notable that these feedback loops are highly sensitive to the concentration of the pathway components, the concentrations of competing species as well as the physical state of the plasma membrane which drives aggregation of the ligand-bound receptor and internalization, the accessibility of PI(4,5)P_2 substrates to PLCβ and PLCδ, and the opening of calcium channels.

Components of the Gαq/PLCβ/PI(4,5)P_2 pathway are also involved in the regulation of membrane tension and cytoskeletal remodeling. The coupling between membrane tension and cytoskeletal adhesion through PI(4,5)P_2 was established nearly two decades ago by Sheetz and coworkers (Raucher et al., 2000; Sheetz, 2001). In a series of elegant experiments, they showed that PIP_2 regulates cytoskeleton-plasma membrane adhesion (Raucher et al., 2000) and that membrane tension plays a critical role in actin remodeling, membrane trafficking, and cell motility (Bittner and Holz, 2005; Diz-Munoz et al., 2013; van Rheenen and Jalink, 2002). Subsequently, researchers have continued to establish and identify increasing roles played by the plasma membrane tension and cortical tension in different cellular reorganization processes (Datar et al., 2019) (Logan and

bioRxiv preprint doi: https://doi.org/10.1101/661975; this version posted June 6, 2019. The copyright holder for this preprint (which was not certified by peer review) is the author/funder, who has granted bioRxiv a license to display the preprint in perpetuity. It is made available under aCC-BY-ND 4.0 International license.

Mandato, 2006; Rangamani et al., 2011). Specifically, in neurons, dynamics of growth cone formation, neurite protrusion, and axonal contractility have been shown to be mechanochemically coupled processes (Franze et al., 2009; Kerstein et al., 2015).

Despite these advances in neuronal biophysics, our understanding of synaptic rupture and neurite retraction remains incomplete especially in terms of the mechanisms that underlie overexcitatory responses. In this study, we set out to investigate the effects of prolonged (i.e. several minutes) agonist stimulation of the Gαq signaling pathway in a model neuronal cell line (PC12). We find that prolonged stimulation results in tension-driven neurite retraction unlike the behavior seen in shorter exposures to neurotransmitters. To understand the factors that underlie the observed neurite retraction, we followed the individual components during the process and developed a mathematical model to predict the effects of calcium stimulation by acetylcholine (ACh) and its extended response on retraction through mobilization of the pathways that impact neurite retraction.

Our predictive models showing that membrane tension and actin reorganization are coupled to calcium dynamics through Gαq/PLCβ/PI(4,5)P_2 were verified in cultured PC12 cells as well as in the neuronal network of the nematode *Caenorhabditis elegans.* The 302 neurons that comprise the nervous system of *C. elegans* have been well characterized and these organisms have been used as models to understand neurite formation and retraction (Carr et al 2016). Because of their optical clarity, *C. elegans* allows us to monitor the effects of acetylcholine stimulation on synapses in real time by microscopy. We find that the *C. elegans* neural architecture exhibits the same retraction behavior when exposed to Gαq agonists showing rupture along the spine in the nerve ring, suggesting that the coupling between membrane tension and calcium dynamics occur on the organism level. Taken together, our studies connect signaling processes with mechanical effects that allow us to predict the signaling conditions that shift from outgrowth and maintenance to retraction.

2. RESULTS

Prolonged exposure to carbachol causes neurite retraction

Cultured PC12 cells differentiate to a neuronal phenotype upon treatment with nerve growth factor (NGF) which initiates activation through TrkA receptors (Greene and Tischler, 1976). This treatment results in growth of neurites from the cell body that extend to roughly 3 times the length of the body over a 36-hr period. These neurites can then connect with neurites from other cells resulting in long tubular structures (Drubin et al., 1985).

Addition of a Gαq agonist to the cells activates PLCβ to catalyze the hydrolysis of PI(4,5)P_2. This hydrolysis releases Ins(1,4,5)P_3 into the cytosol that then binds to Ins(1,4,5)P_3 receptors on the ER to release calcium from intracellular stores. In addition to eliciting calcium signals, PI(4,5)P_2 hydrolysis can exert mechanical effects on cells by altering membrane tension and actin-membrane adhesion (Sheetz, 2001) (Logan and Mandato, 2006; Raucher et al., 2000). We sought to understand the interactions between the Gαq/PLCβ pathway and mechanical features of membrane-actin interaction **(Fig. lA, B).**

We found that when we add a Gαq agonist, such as carbachol or bradykinin, to PC12 cells,

bioRxiv preprint doi: https://doi.org/10.1101/661975; this version posted June 6, 2019. The copyright holder for this preprint (which was not certified by peer review) is the author/funder, who has granted bioRxiv a license to display the preprint in perpetuity. It is made available under aCC-BY-ND 4.0 International license.

the well-formed neurites become thinner, their connections rupture (compare **Fig lC to Fig. lE, S1)** and they retract toward the soma after a period of 5-10 minutes **(Fig. lE, F).** After retraction, the excess membrane appears as blebs around the sides of the cell **(Fig. lG).** This behavior was seen in every cell viewed in over 100 experiments, but was not seen when a PLCβ inhibitor was added, or a Gαi agonist, such as isoproterenol was used. The initiation and rate of retraction depended on the particular treatment and condition of the experiment, as described below. The extent of retraction in a specific time period was robust to the length and thickness of the neurite.

Neurite retraction is coupled with Gαq/PLCβ/calcium pathway

We followed the activation of the Gαq/PLCβ/calcium signaling pathway upon stimulation in single PC12 cells using the fluorescent calcium indicator, Calcium Green, to determine whether neurite retraction is concurrent with activation. Our approach was to follow some of the molecular constituents of the Gαq pathway and determine the temporal correlation between activation of the individual signal components and neurite retraction. The retraction velocities of a generic Gαq-coupled receptor (i.e. the bradykinin receptor type 2 or B2R) were measured by transfecting cells with a fluorescent-tagged construct and stimulating the cells with agonist (i.e. bradykinin). We note that B2R is not endogenous to PC12 cells, thus allowing us to compare Gαq-associated retraction with those that result from stimulation of endogenous muscarinic receptors. We find identical retraction behavior for neurite retraction after stimulating the B2R transfected cells with bradykinin as those that result from carbachol stimulation **(Fig. 2).** These results support a connection between neurite retraction and Gαq/PLCβ activation.

We calculated the velocity of neurite retraction by analyzing the decrease in length of each neurite at each time point during the experiment (see *Methods*). These velocities were analyzed for PC12 cells transfected with eCFP-B2R *(blue)* and for the plasma membrane *(orange)* as monitored by the phase contrast imaging (**Fig. 2A**). We find that the velocity of retraction of the plasma membrane is more gradual than that of the receptor suggesting that movement of the receptor towards the soma precedes the membrane.

Activation of the PLCβ pathway through Gαq-GPCRs results in hydrolysis of the signaling lipid PI(4,5)P_2. We followed the change in the level and distribution of PI(4,5)P_2 of the plasma membrane surrounding the soma and neurite during retraction using a fluorescent PI(4,5)P_2 sensor (i.e. eGFP-PH-PLCδ1). Our data show that PI(4,5)P_2 moves from the neurite into the soma with a similar retraction velocity as the GPCR **(Fig. 2E).** However, this movement is oscillatory showing three precipitous drops and recovery during the retraction event. These are three distinct movements of PI(4,5)P_2 during the observed retraction occur at similar times (~3, 10 and 15 min) for all cells tested, and are interpreted as being due to PI(4,5)P_2 replenishment during the course of the retraction.

In general, Gαq activation produces an increase in the calcium typified by an initial spike in the first few minutes followed by a slow recovery. We followed the calcium behavior upon stimulation in single cells using a fluorescent calcium indicator, Calcium Green **(Fig 1D, F, H** and **2J).** Correlating calcium responses with neurite retraction shows that retraction occurs even in this initial phase and continues through the duration of the recovery phase.

We constructed a spatial model of the Gαq/PLCβ/PI(4,5)P_2 signaling pathway using reaction-diffusion equations. The reactions, kinetic parameters, and diffusion constants are given in **Tables S1-4** in the Supplementary Material (*SOM*). The soma of the PC12 cell was modeled as a sphere with a cylindrical neurite as a simplified geometry capable of capturing the key features of these cells. Briefly, the soma was modeled as a sphere with a radius of 5 μm, and the neurite was modeled as a cylinder

bioRxiv preprint doi: https://doi.org/10.1101/661975; this version posted June 6, 2019. The copyright holder for this preprint (which was not certified by peer review) is the author/funder, who has granted bioRxiv a license to display the preprint in perpetuity. It is made available under aCC-BY-ND 4.0 International license.

with a radius of 1.25 μm and length of 30 μm. The endoplasmic reticulum was modeled as a cylinder with a radius of 0.25 μm and length of 25 μm, and the nucleus as a sphere with a radius of 2 μm. Geometric details are given in **Table S5**. The nucleus was treated as an excluded volume, while the ER was treated as a calcium source. Computational modeling of this pathway in a three-dimensional spatial model using finite elements captured the calcium transients with the same time scale as the experiments (compare **Fig. 2J** and **Fig. 2K).** This framework sets the stage for the mechanical coupling of calcium dynamics to neurite retraction.

Actin remodeling proteins affect the dynamics of neurite retraction

Actin filaments are the major cytoskeletal components of synapses and are the key modulators of neurite plasticity. An actin filament is a dynamic structure in which monomers disassemble from one end and reassemble on the other; a behavior knows as molecular treadmilling. Retraction involves inward movement of the actin structure that defines the neurite shape and so any model of retraction must incorporate actin disassembly. In neurites, actin filament remodeling is known to be associated with the drag forces related to protrusion (Datar et al., 2019). Additionally, PI(4,5)P_2 hydrolysis is closely connected to membrane-actin adhesion and membrane tension regulation (Raucher et al., 2000).

Based on our experimental observations **(Fig. 2),** we coupled PI(4,5)P_2 hydrolysis and calcium release following carbachol-stimulation with a mechanical model that balances the forces due to actin depolymerization and membrane cortical tension change. Due to the timescale separation between the biochemical signaling dynamics and neurite retraction, we coupled the 3D spatial model of the Gαq/PLCβ/calcium signaling pathway **(Fig. lA-B)** to an ordinary differential equation model of neurite mechanics, assuming uniform signaling dynamics at extended timescales (Section **S1-2** in *SOM*). Briefly, the mechanical model proposes a force balance acting on the tip of the neurite (Hassinger et al., 2017). The force due to the actin cytoskeleton is acting outward, away from the soma and the force exerted by the membrane cortical tension is acting towards the soma. In this case, we assume that the cortical tension is a function of the change in the area of the membrane. This change in membrane area can result from PI(4,5)P_2 hydrolysis (Raucher et al., 2000; Sheetz and Dai, 1996), from endocytosis of GPCRs (Getz et al., 2019) and from changes in tension (Simunovic et al., 2017). The force exerted by the actin cytoskeleton is modeled phenomenologically as a function of calcium-mediated cofilin and retrograde flow (Bornschlogl et al., 2013). Thus, the net force balance can be written as:

$$\underbrace{-F_{tension}}_{\text{Force due to cortical membrane tension}} + \underbrace{F_{actin}}_{\text{Force due to actin dynamics}} = \underbrace{\frac{\eta}{k_L L}\frac{dL}{dt}}_{\text{Drag forces}} \quad (1),$$

where

$$\eta = \underbrace{\mu_e}_{\text{drag coefficient for external fluid}} + \underbrace{\frac{\mu_m}{\delta}}_{\text{drag coefficient for membrane}} \quad (2).$$

Modeling the neurite as a cylinder with a hemispherical end cap, we obtain the governing equation for the length of the neurite as

bioRxiv preprint doi: https://doi.org/10.1101/661975; this version posted June 6, 2019. The copyright holder for this preprint (which was not certified by peer review) is the author/funder, who has granted bioRxiv a license to display the preprint in perpetuity. It is made available under aCC-BY-ND 4.0 International license.

$$\underbrace{\frac{dL}{dt}}_{\text{rate of change of neurite length}} = \underbrace{\frac{k_L L}{\eta}}_{\text{drag coefficients and length effects}} \underbrace{(-F_{tension} + F_{actin})}_{\text{Forces}} \quad (3).$$

This governing equation combines the force balance above with experimental observations that retraction velocity is proportional to neurite length. The force due to membrane cortical tension and actin dynamics depend on equations for τ and F_{actin}, respectively, given as

$$\frac{d\tau}{dt} = \underbrace{\frac{dArea}{dt}(f(PIP_2))}_{\substack{\text{area change} \\ \text{with PIP2 dependence}}} \underbrace{F_{perPIP_2}}_{\substack{\text{tension change} \\ \text{per PIP2}}} \underbrace{\frac{k_{tension}}{A_0}}_{\text{unit correction}} \quad (4),$$

and

$$\frac{dF_{actin}}{dt} = \underbrace{\frac{F_{perActin} k_{actin}}{L_0}}_{\substack{\text{Force and length} \\ \text{effects}}} \underbrace{(k_{const} + k_{cofilin} + k_{actin} + k_{drebrin})}_{\text{k contributions}} \frac{dL}{dt} \quad (5).$$

This is a phenomenological model with a combination of parameters from literature and constants fit to the experimental results, *(see SOM)*. In particular, Eqs. (4) and (5) have dependence on f(PIP2) and g(CofilinAct), which are sigmoidal functions that trigger in response to PI(4,5)P2 and activated cofilin, respectively(Zmurchok et al., 2018).

Using this model, we simulated calcium-mediated neurite retraction in control cells. We found that the model is able to capture the dynamics of neurite retractions events **(Fig. 3C).** These models utilized experimental retraction data collected using differentiated PC12 cells transfected with low amounts of mCherry-actin to fit the phenomenological constants **(Fig. 3)**. Effectively, the model predicts that when the force exerted by actin is matched by the force due to tension, there is no change in the length of the neurite. Upon increase in PI(4,5)P_2 hydrolysis and calcium release into the cytosol, the forces due to membrane cortical tension increase while the forces exerted by the actin decrease and the neurite pulls back.

If this prediction is true, then we should be able to alter neurite retraction behavior by altering the expression of actin-related proteins or by membrane tension separately. We next probed neurite retraction dynamics by varying the concentration of select actin-related proteins such as cofilin, drebrin, and actin itself both in experiments and modeling.

Actin modulators regulate neurite retraction velocity

We followed actin disassembly in real time during carbachol-stimulated retraction using mCherry-actin in control cells and cells over-expressing cofilin or drebrin **(Fig. 4).** Cofilin increases severing of actin filaments increasing actin filament breakdown while drebrin stabilizes actin filament inhibiting disassembly (Calabrese et al., 2014; Grintsevich and Reisler, 2014; McCullough et al., 2008; Mikati et al., 2013). **Fig. 4 D-L** are screen shots of the time lapse video made during retraction where **Fig 4. D-F** are representative cells prior to stimulation with carbachol, **Fig. 4G-I** show the same cells at the beginning of retraction, and **Fig. 4J-L** show the cells at longer times. Movies of retraction *(SOM2)* were analyzed to obtain the retraction velocities during the three different conditions **(Fig. 4M-P).** This quantification enables the comparison of neurite retraction dynamics of actin in our control versus actin when cofilin and drebrin are overexpressed. As expected, overexpression of cofilin enhances the rate of neurite

bioRxiv preprint doi: https://doi.org/10.1101/661975; this version posted June 6, 2019. The copyright holder for this preprint (which was not certified by peer review) is the author/funder, who has granted bioRxiv a license to display the preprint in perpetuity. It is made available under aCC-BY-ND 4.0 International license.

retraction **(Fig. 4M** versus **Fig. 4N),** and complete retraction results in cells with a trapezoidal morphology rather than the circular one typified of undifferentiated PC12 cells. This altered morphology likely stems from the lower number of actin filaments throughout the cell due to cofilin overexpression (Pavlov et al., 2007).

We expected that transfection of the cells with drebrin would strongly impede neurite retraction in the presence of carbachol because drebrin is known to bind assembled actin filaments (F-actin) and stabilize them (Mikati et al., 2013; Nair et al., 2017; Sharma et al., 2011). Low amounts of actin allowed a sustained linear decrease **(Fig. 4O)** whose compiled average is within error of mCherry-actin along **(Fig. 4P).** These data support the idea that disruption of the intact actin network and its dynamic modeling when impeded by cofilin overexpression (increased severing) or by drebrin overexpression (inhibition of disassembly and remodeling) are key driving forces in governing retraction dynamics.

We modeled overexpression of cofilin, drebrin, and actin in the mechanical framework by altering the F_{actin} terms *(Eq.* 5) to represent the known effects of these proteins through the 'k' contributions for each protein. We modeled actin force overall as a stress-strain relationship, where the 'k' terms captured the contribution of each protein to overall actin force dynamics. For example, cofilin expression was incorporated in our constitutive equation as an increase in the total cofilin available for calcium activation, which therefore causes a faster decrease in F_{actin} by increasing the magnitude of the rate of change of F_{actin} through the $k_{cofilin}$ term. As a result, our model predicts that neurite retraction velocity is faster for cofilin overexpression compared to control **(Fig. 4R,V).** Similarly, we modeled drebrin overexpression by increasing drebrin concentration within the $k_{drebrin}$ term, consistent with experimental observations that a higher drebrin concentration slows actin depolymerization and thus slows the decrease in F_{actin} (Mikati et al., 2013; Sharma et al., 2011). Therefore, our model predicts that drebrin overexpression slows neurite retraction velocity compared to control **(Fig. 4S,W).** Actin overexpression can be modeled in a similar fashion as drebrin and is captured through the k_{actin} term. Thus, increasing actin concentration is essentially increasing the actin-to-cofilin ratio and therefore slowing the decrease in F_{actin}. Our model predicts that actin overexpression will slow neurite retraction velocities compared to control **(Fig. 4Q,U).**

The results in **Fig. 4** show that by varying cofilin, drebrin, and actin concentrations, we predict different actin force dynamics that translate to different neurite retraction rates. Specifically, we predict that cofilin, actin, and drebrin overexpression leads to more rapid, slower, and slightly slower neurite retraction velocities compared to control, respectively. Our modeling results agree with the experimental observations and suggest that actin disassembly and inhibition of reassembly are necessary for retraction. To support these studies, we quantified experiments that measured retraction of control cells and cells that overexpress actin, cofilin and drebrin. The experimental velocities of the retractions are plotted in **Fig. 4P** and validate our model predictions in **Fig. 4X**.

Neurite retraction can be driven by membrane tension.

Given that there are two contributions to the force acting on the neurite, one from actin and the other from membrane cortical tension, we next asked whether neurite retraction could be driven by changes to the membrane cortical tension alone. We directly tested this idea using hyper-osmotic stress to increase membrane tension. Increasing the hyperosmotic stress from 300 to 600 mOsm on cultured PC12 cells resulted in the same retraction behavior and timescale as seen with carbachol stimulation **(Fig. 5A).** To determine the change in membrane tension induced by this change in osmolarity, we measured tension by atomic force microscopy (AFM). This method allows

bioRxiv preprint doi: https://doi.org/10.1101/661975; this version posted June 6, 2019. The copyright holder for this preprint (which was not certified by peer review) is the author/funder, who has granted bioRxiv a license to display the preprint in perpetuity. It is made available under aCC-BY-ND 4.0 International license.

us to assess the stiffness of cells by measuring the amount of deflection experienced by a cantilever with known spring constant as it indents the surface of the cell. For undifferentiated, differentiated, and retracted PC12 cells, AFM measurements were taken at the base of the neurites or retracted neurites. The stiffness of each cell was determined by averaging the stiffness values at three separate locations on each cell in order to combat the inherent heterogeneity in cell structure while ensuring no localized damage from a previous measurement. Undifferentiated cells were the stiffest condition tested, followed by retracted and then differentiated **(Fig. 5B).**

We also used AFM to determine the stiffness of cells subjected to hypo-osmotic and hyper-osmotic stress for undifferenced and differentiated PC12 cells. Hypo-osmotic and hyper-osmotic stress, which leads to cell swelling and cell dehydration respectively, results in an increase and decrease in cell stiffness, respectively **(Fig. 5B).** Force curves that are representative of the average stiffness value for each condition show a smooth Hertz model relationship between indentation depth and applied force as expected **(Fig. 5C-D).** Taken together, these studies show a direct correlation between cell stiffness and osmotic stress, which is also correlated to retraction.

Within our model, we can also probe neurite retraction dynamics by varying the contribution of tension, the τ component, of the mechanical model. Membrane cortical tension is altered under hyperosmotic conditions when water expulsion from the cell leads to a reduction in volume-to-surface area ratio. Therefore, to model hyperosmotic conditions instead of a carbachol stimulus, we predict that this volume-to-surface area ratio change causes an increase in membrane cortical tension**.** Therefore, we model a slightly elevated membrane cortical tension initial condition that triggers a related force (**Fig. 5E**) and neurite retraction (**Fig 5F).** We also see a change in actin force, triggered due to the coupling between actin and tension in the model, which is also predicted experimentally due to the necessary actin reorganization during retraction caused by hyperosmotic conditions. Therefore, our model predicts neurite retraction in the absence of a ligand stimulus with hyperosmotic conditions **(Fig. 5F),** indicating that membrane cortical tension is a key component governing neurite retraction dynamics.

We tested whether the retraction that results from osmotic stress is convergent with the Gαq/PLCβ pathway. Keeping in mind that membrane compression regulates calcium flux to drive actin dynamics in model systems (Hartzell et al., 2016; He et al., 2018; Nourse and Pathak, 2017), we determined whether hyper-osmotic stress will open calcium channels to allow divalent cation influx to relieve the osmotic stress. Using a fluorescence calcium indicator, we found that increasing the osmotic strength from 300 to 600 mOsm results in a small increase in intracellular calcium that is ~10% of the increase seen for ACh stimulation. To verify that calcium is mediating retraction, we removed extracellular calcium from the media and found that even though increasing the osmotic strength through the addition of KCl caused membrane folds and puckering, consistent with a loss in cell volume, neurite length remained constant (**Fig. 5G**). This result indicates that the two types of retraction pathways converge on calcium levels, those initiated by Gαq/PLCβ stimulation and those initiated by extracellular calcium influx by tension sensitive calcium channels.

Prolonged exposure to Gαq agonists leads to nerve ring disruption in *C. elegans*

To determine whether we could disrupt neuronal connections and retract neurites in a neuronal network, we used the optically clear model system, C. *elegans.* We first used a strain of *C. elegans* (QW1166) that expresses an integrated fluorescent calcium sensor G-CaMP throughout the nervous system. This system allows us to visualize by fluorescence, the neurons that show increased calcium levels in response to acetylcholine stimulation. This specific strain has fluorescence in every neuron in the nerve ring allowing us to look at the ring as a whole, as well as fluorescence in the entire ventral nerve of the worm that extends the entire length of the worm.

bioRxiv preprint doi: https://doi.org/10.1101/661975; this version posted June 6, 2019. The copyright holder for this preprint (which was not certified by peer review) is the author/funder, who has granted bioRxiv a license to display the preprint in perpetuity. It is made available under aCC-BY-ND 4.0 International license.

We focused on acetylcholine signals emanating from neurons within the nerve ring located in the head of the worm and along the ventral nerve cord **(Fig 6A).** Normal signal transmission can be seen in the images in **Fig 6B.** For these studies, we only wished to determine whether there is broad neuronal rupture and retraction within the nerve ring and along the ventral nerve which would be indicated by the lack of fluorescence in the center in the ring and dark spots along the ventral nerve. In every worm tested (n=10), we find neuronal rupture with acetylcholine stimulation that occurs in the nerve ring close to the organism's mouth **(Fig. 6C).** Additionally, we see a distinct pilling of the ventral nerve that displays thinning and clustering, and portions that are no longer fluorescent indicting large-scale neuronal damage.

We confirmed the connection between neuronal network disruption produced by extended acetylcholine stimulation to membrane tension by subjecting the worms hyper-osmotic stress (increasing the salt solution concentration by 50%). After osmotic stress, these organisms showed a lack of fluorescence in the nerve ring indicating rupture and retraction of neurons. Also, we see much larger segments of the ventral nerve that have been disrupted with less pilling than that seen for acetylcholine stimulation **(Fig. 6D).** The somewhat different morphological effects on the ventral nerve seen in osmotic stress is most likely due to the ability of the stress to be distributed uniformly along the length of organism as opposed to carbachol whose receptors are concentrated mostly in the mouth.

To support neuronal disruption of the worms by acetylcholine, we followed changes in movement of the whole organisms using a chemotaxis assay with and without acetylcholine stimulation. These studies were also done using the *C.elegans* QW1166 strain. We see that after treatment with acetylcholine 83% of the worms moved towards the attractant while the remaining 17% did not move at all **(Fig. 6F).**

DISCUSSION:

In order for an organism to learn, neurons must break and reform connections with neighboring neurons and disruptions in these processes underlie learning-based neurological diseases and neurodegeneration. Despite the importance of synapse severing and formation, the mechanisms that underlie neural plasticity are not well understood (Licht et al., 2011)(Wu 1996). Previous studies of neural plasticity have mainly focused on contributors to neurogenesis in hippocampal neurons and cultured drosophila neurons, such as neuronal stem cells (LaFerla, 2002). Here, we have defined the synaptic breakage and neurite rupture in neural plasticity in terms of membrane tension and calcium-induced retraction that will allow for predictable actin remodeling.

Calcium is a crucial component for the growth, differentiation, and survival of neurons (Spitzer 2011). Calcium helps to regulate the differentiation of specific neuronal types as well as their migration through the body, and calcium levels are directly liked to neurodegenerative diseases such as Alzheimer' s (LaFerla, 2002). We followed neuronal cell response to extended calcium signals that may mimic dysfunctional states. Unexpectedly, we find that extended calcium levels resulted in complete neurite retraction, and this retraction can be seen by following the plasma membrane, by a GPCR coupled to Gαq, and by $PI(4,5)P_2$. These data show that the Gαq signaling pathways are intimately involved with the mechanical properties of the cell.

The connection between calcium signals from GPCR/Gαq and cell mechanics was supported using fluorescent-tagged actin and by measuring retraction when overexpressing

bioRxiv preprint doi: https://doi.org/10.1101/661975; this version posted June 6, 2019. The copyright holder for this preprint (which was not certified by peer review) is the author/funder, who has granted bioRxiv a license to display the preprint in perpetuity. It is made available under aCC-BY-ND 4.0 International license.

cofilin, an actin depolymerizing protein, or drebrin, an actin monomer recruitment protein. Overexpressing cofilin at a level 6x higher than endogenous levels allows for much faster velocities of neurite retraction initiated by GPCR-Gαq/Ca^{2+} after an initial lag period. These observations correlate well with cofilin's ability to depolymerize actin, but shows that activation of the Gαq/PI(4,5)P_2/Ca^{2+} pathway is a necessary prerequisite. In contrast, cells overexpressing drebrin show a similar retraction rate as endogenous which correlates to its ability to stabilize actin monomers (Mikati et al., 2013). This observation indicates that the behavior we are viewing is solely due to actin depolymerization without contributions of the polymerization events. Thus, while Ca^{2+} signals drive retraction, actin plays a passive role.

The coupling between calcium signaling and mechanical forces has been observed in cell motility and in dendritic spines during long-term potentiation, astrocyte calcium signaling, and during neurite protrusion and formation (Mutalik et al., 2018). Based on these studies, we postulated that neurite retraction results from changes in cortical tension brought about by receptor endocytosis, PI(4,5)P_2 hydrolysis and IP_3 generation, and an increase in intracellular calcium, and formulated a mechanochemical pathway to test this idea. We found that indeed, a force balance between cortical tension and actin-mediated forces, both of which are mediated by intracellular calcium levels, is sufficient to capture the dynamics of neurite retraction. This idea was explicitly tested by measuring changes in membrane stiffness with osmotic strength and by altering the effects of different actin remodeling proteins. We also found that the effects of actin and cortical tension could be uncoupled to a certain extent, pointing towards multiple mechanical pathways that could exquisitely regulate neurite retraction. We acknowledge that the proposed model is phenomenological, and while it captures the key physics of the processes underlying neurite retraction, future studies will focus on elaborating on some of the phenomenological relationships proposed here.

Our results show that calcium signals may have a dramatic impact on neuronal morphology and synaptic connections, and this idea was demonstrated in *C. elegans*. Neurite formation and extension is essential to transition from neuroblast to mature neuron and *C. elegans* are an excellent model system to understand neurite formation and retraction (Carr et al 2016). The site of nascent neurite outgrowth is determined by cell intrinsic factors that orchestrate the localized regulation of actin and microtubules (van Beuningen SFB, 2015, Flynn KC, 2012) and in developing neurons, these factors are polarized at sites of neurite outgrowth in response to extracellular cues (Adler CE, 2006, Randlett O 2011). Our finding that the neural network of this organism can be modified by Gαq activation or increased mechanical tension, may form a basis for studies that better describe neural rewiring paradigms.

In summary, our studies indicate the role of acetylcholine in facilitating neurite retraction. Further research on how this pathway interacts with other pathways to coordinate remodeling with such spatio-temporal precision will provide insights into understanding the molecular basis of neurodegeneration.

ACKNOWLEDGEMENTS

This work was supported by NIH GM116187 (SS) and AFOSR MURI FA9550-18-1-0051 (PR). We thank various members of the Rangamani and Scarlata labs for valuable discussion and manuscript review. We would like to thank the UCSD Interfaces Graduate Training Program and the San Diego Fellowship for funding and support for MB. MB was also supported by AFOSR MURI grant number FA9550-18-1-0051 to PR and a grant from the National Institutes of Health, USA (NIH Grant T32EB009380).

bioRxiv preprint doi: https://doi.org/10.1101/661975; this version posted June 6, 2019. The copyright holder for this preprint (which was not certified by peer review) is the author/funder, who has granted bioRxiv a license to display the preprint in perpetuity. It is made available under aCC-BY-ND 4.0 International license.

MATERIALS AND METHODS

Cell Culture, transfection and differentiation

PC12 cells, which are derived from rat pheochromocytoma (ATCC CRL-1721), were cultured in 35mm or 100mm poly-d-lysine coated petri dishes using Dulbecco's Modified Eagle's Medium (DMEM) (Gibco) with 10% heat-inactivated horse serum (Gibco), 5% fetal bovine serum (Atlanta Biologicals), and **1**% penicillin/streptomycin. The dishes were incubated with 5% CO_2 at 37°C. Cells were transfected using different amounts of plasmid based on the concentration tested using a NanoDrop. Cells were transfected using Lipofectamine 3000 (Invitrogen) following the protocol of the manufacturer. The media used in transfection was the same DMEM culture media with the exception of antibiotics, to increase transfection efficiency and the media was changed back to normal culture media after 24 hours. Cells were differentiated using media that contained DMEM, 1% heat-inactivated horse serum and 1% penicillin/streptomycin. Added to this would be a 1 to 1000 ratio of l00ng /µl nerve growth factor (NGF) (Novoprotein). This media is added to the cells for at least 48 hours and up to 96 hours to achieve long neurites.

Plasmids and Maxi/Mini prep

Fluorescent-tagged plasmids were obtained and maxi/min prepped using Qiagen kit and following the manufactures guidelines. The plasmids were obtained from Addgene. Actin #54967 derived by Michael Davidson at Harvard Medical School, Drebrin #40359 derived by Phillip Gordon-Weeks at King's College of London, Cofilin #51279 derived by James Bamburg at Colorado State University, Pleckstrin homology (PH)-domain of PLC8 # 21179 derived by Tobias Meyer at Stanford University, and the bradykinin type 2 receptor was modified from the construct provided by Porf. Leed-Lundber, Univ Texas San Antonio.

Calcium Green Staining

Prior to imaging, cells are washed with HBSS and then a 1/200 mixture of HBSS and Calcium Green (Thermofisher) is added and allowed to incubate for **1** hour before imaging.

Preparation of Carbachol

Carbachol in powdered form was obtained from Sigma Aldrich. It was dissolved in water to a final concentration of l mM at a volume of l0 mL and aliquoted into 500µL portions to be used for each experiment. The solutions were kept at -20°C.

Fluorescent Microscopy/ Stimulation of Cells

Fluorescent imaging was done using a Zeiss LSM510 inverted confocal microscope. Imaging was carried out at least 48 hours post transfection and differentiation. The cells were grown and imaged in a MAT-Tek 8 chamber glass bottom plates or a MAT-Tek 35mm glass bottom dish. Once a single cell was found visually that expressed the plasmid or stain, the microscope would be switched to the correct wavelength and laser intensity. A time series image was then started and stopped after 10 frames, the cells would then be manually stimulated by adding carbachol to the dish to achieve the desired final molarity, and the time series video was then started immediately after adding the Carbachol.

Osmotic Stress and EDTA studies

Osmotic stress studies were done using calcium free isotonic media for imaging with the

bioRxiv preprint doi: https://doi.org/10.1101/661975; this version posted June 6, 2019. The copyright holder for this preprint (which was not certified by peer review) is the author/funder, who has granted bioRxiv a license to display the preprint in perpetuity. It is made available under aCC-BY-ND 4.0 International license.

addition of KCl at different concentrations to achieve osmotic stress. Studies that include EDTA, (J.T. Baker) cells were osmotically stressed and EDTA was added to the dish to give a final concentration of 0.5 for partial neurite retraction and 1μM for full neurite retraction.

Plasmid-specific studies

Calcium green and enhanced green fluorescent protein (eGFP) studies were imaged using an argon laser at 488nm. Red fluorescent protein (RFP) and mCherry were imaged using argon ion and HeNe lasers at 543nm. YFP and CFP were imaged using argon ion and HeNe lasers at a wavelength of 545nm. Multi-track imaging can also be done combining each of these set ups. Images were taken by alternating between probes when data for more than one are being monitored, and these images are subsequently merged.

Atomic Force Microscopy Stiffness Measurements

Live cells were probed utilizing an MFP-3D-BIO atomic force microscope (Asylum Research) and a DNP cantilever (Bruker) with nominal spring constant 0.06 N/m[1]. The cantilever was calibrated before each measurement to ensure accuracy. Cells were seeded on 60 mm poly-d-lysine coated petri dishes using Dulbecco's Modified Eagle's Medium (DMEM) (Gibco) with 10% heat-inactivated horse serum (Gibco), 5% fetal bovine serum (Atlanta Biologicals), and 1% penicillin/streptomycin. After 24 hours of recovery cells were differentiated using media containing DMEM, 1% heat-inactivated horse serum and 1% penicillin/streptomycin. Added to this would be a 1 to 1000 ratio of lO0ng/μl nerve growth factor (NGF) (Novoprotein). This would be added to the cells a minimum of 24 hours before measurements are taken.

Cells were viewed two days after plating and one day after treatment with nerve growth factor (NGF). Cells with minimal cell-cell contact were selected to reduce the mechanical impacts of cell communication. Three force curves in separate perinuclear regions with cantilever velocity of 2μm/s and trigger point lnN were taken for each selected cell. Measurements were taken within 30 minutes of removal from the incubator to facilitate cell viability.

The stiffness of the measured cells ***E*** was determined from the force curve data utilizing the Hertz model for conical cantilever tip geometry:

$$\boldsymbol{E} = \mathrm{Kddrr}(1\text{-}v^2)/\ 2\mathrm{Ll}^2 \tan c/J$$

where ***k*** is the cantilever spring constant, dis the cantilever deflection, vis the poison's ratio (0.5 used for an assumed incompressible material), ***A*** is the sample indentation depth, and ***<P*** is the half-angle of the conical cantilever tip (35°). The force curves were processed using a custom MATLAB code that fits the indentation curve over a 500nm range after manual selection of the initial contact point.

Fluorescent Imaging of C. elegans

Worms were transferred into a microcentrifuge tube containing l mM carbachol and were submerged in the tube for 30 minutes at room temperature or 100mM NaCl solution for 10 minutes. After 30 or 10 minutes respectively, the worms were removed from solution and placed on a glass slide with a thin layer of agar on it for the worms to lay on. Excess carbachol was wicked up from the pad and the worms were paralyzed using 25M levamisole that does not a affect our pathway of interest. The worms were then imaged on an inverted confocal microscope and were visually checked for neurite rupture and retraction.

Chemotaxis Assay of C. elegans

bioRxiv preprint doi: https://doi.org/10.1101/661975; this version posted June 6, 2019. The copyright holder for this preprint (which was not certified by peer review) is the author/funder, who has granted bioRxiv a license to display the preprint in perpetuity. It is made available under aCC-BY-ND 4.0 International license.

Worms were transferred to a new seeded plate 24 hours prior to the experiment. The day of the experiment an unseeded plate is marked with a dot in the center and two circles on either ends of the plate with the "C" for control of DI water and "D" for diacetyl which is the attractant**.** Using approximately 1mL of s. basel the worms are washed into a microcentrifuge tube and allowed to pellet for 5-10 minutes. Once pelleted, the worms are washed with s. basel two more times and finally with water. 10µL of the suspended worms are transferred to the experimental plate previously made and the excess water is removed by wicking. The plate is then incubated for 45 minutes at 20ºC, and after, the number of worms that have moved either to the attracted or control is counted.

bioRxiv preprint doi: https://doi.org/10.1101/661975; this version posted June 6, 2019. The copyright holder for this preprint (which was not certified by peer review) is the author/funder, who has granted bioRxiv a license to display the preprint in perpetuity. It is made available under aCC-BY-ND 4.0 International license.

Figure 1: Neurite retraction in PC12 cells is induced by calcium stimulation.

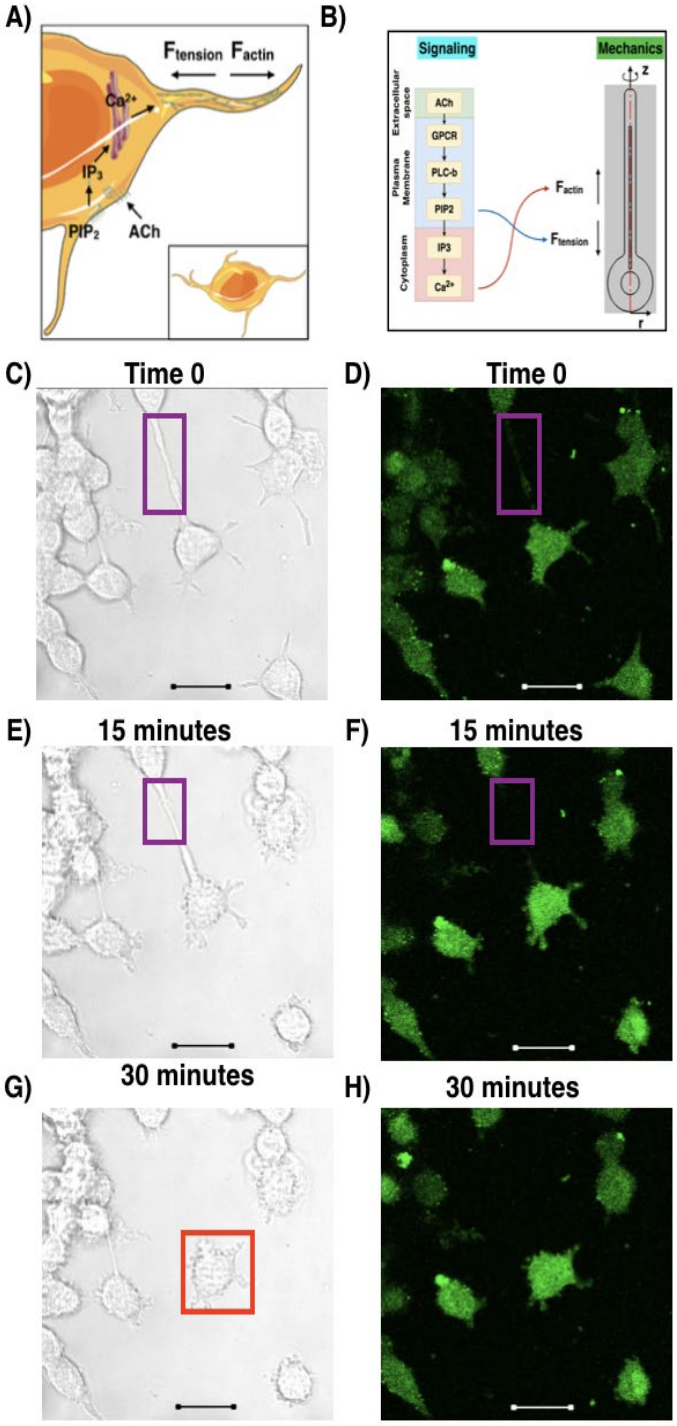

A) *Cartoon of the mechanochemical events underlying neurite retraction in a PC12 cell.* The figure depicts the interconnection between calcium signaling and force regulation due to membrane cortical tension and actin remodeling. **B)** *Schematic showing the coupling between signaling and mechanical changes within the PC12 cell.* We identify membrane cortical tension and actin dynamics as key players controlling neurite retraction rates, and link calcium dynamics to actin reorganization and force generation, and PI(4,5)P_2 hydrolysis to membrane tension change and tension force generation. Using this coupled model, we are able to reproduce the neurite retraction behavior observed experimentally. **C-D)** *Sample images of differentiated PC12 cells before stimulation.* Confocal phase contrast **(C)** and fluorescence images of cells loaded with a fluorescent calcium sensor, Calcium Green, are shown **(D)**. **(E-G)** *Stimulation of cells with carbachol results in neurite thinning, retraction and synaptic rupture.* 15 minutes after the addition of carbachol, we observe membrane retraction (e.g. purple box), and thinning of the neurite (**E-F**). 30 minutes after carbachol addition, we see a complete retraction of the neurites into the soma and membrane blebbing at the retraction sties (e.g. red box) (**G-H**). In all images, the scale bar is 20µm. Identical behavior was seen in 20 cells.

bioRxiv preprint doi: https://doi.org/10.1101/661975; this version posted June 6, 2019. The copyright holder for this preprint (which was not certified by peer review) is the author/funder, who has granted bioRxiv a license to display the preprint in perpetuity. It is made available under aCC-BY-ND 4.0 International license.

Figure 2 Neurite retraction of PC12 cells upon Gαq stimulation.

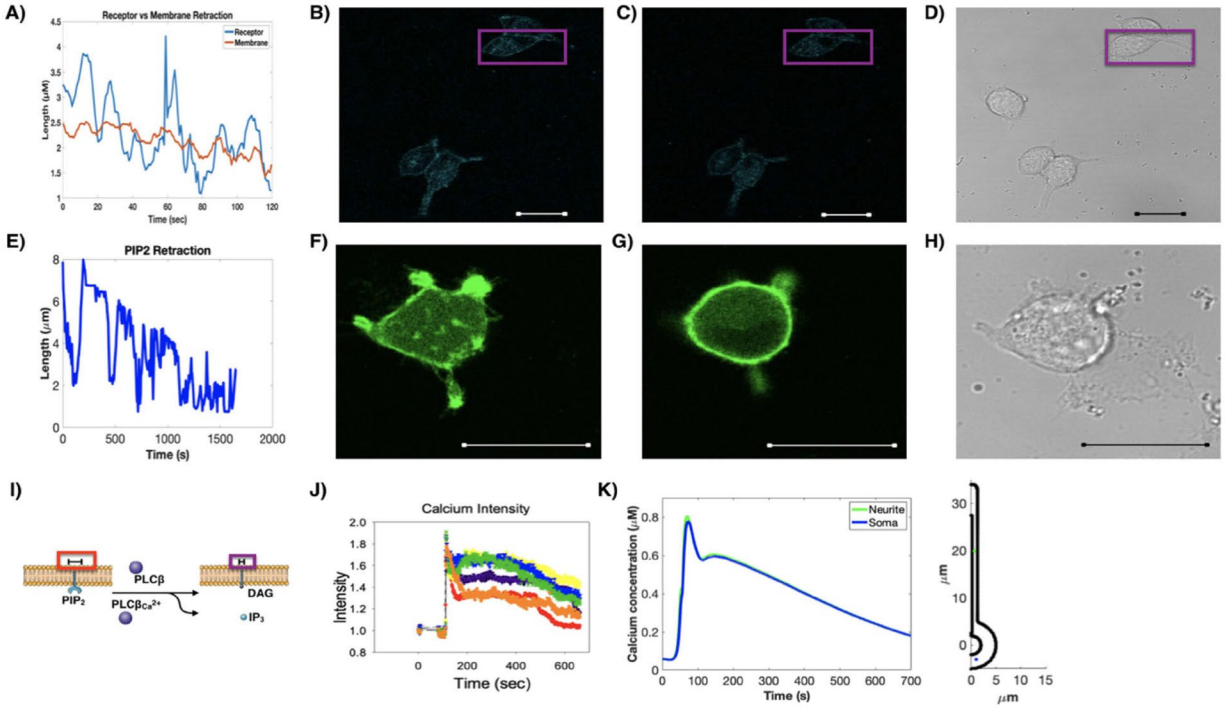

A) Decrease in neurite length of the B2R receptor in PC12 cells (blue) as compared to slow reduction in length of the membrane as followed by phase contrast (orange). **B)** Images of differentiated PC12 cells expressing eCFP-B2R prior to stimulation with bradykinin and **(C)** 30 minutes after stimulation where purple box shows the retraction data of **(A)**, and the corresponding phase contrast image is shown in **(D)**. **E)** Decrease in neurite length as followed using a fluorescent PI(4,5)P_2 sensor, PH-PLCδ1 (Garcia et al., 1995) where distinct oscillations are seen. **F)** Images of a differentiated PC12 cells expressing PH-PLCδ1, prior to stimulation, **(G)** 30 minutes after stimulation with carbachol, and **(H)** the corresponding phase contrast image are shown. **I)** Cartoon showing the hydrolysis of PI(4,5)P_2 to Ins(1,4,5)P_3 and DAG depicting the larger head group of PIP_2, denoted by the scale bar (red box), as compared to the smaller DAG that remains in the membrane after hydrolysis, (purple box). This decrease in the size of the membrane bound molecule (PI(4,5)P_2 to DAG) leads to a local change in tension (denoted by the scale bars). IP_3 moves into the cytosol and to the ER, causing a release of calcium. **J)** Graph of calcium intensity in neurites of six different cells. This graph shows the lag time after the addition of carbachol, the initial spike in calcium and the slow recovery. **K)** Model replicating the intensity of calcium over time at two spatial locations (in the neurite and in the soma) after stimulation by carbachol. *Inset*: location of traces within the model geometry (in the neurite and in the soma). In all images, the scale bar is 20μm, and n>15 cells.

bioRxiv preprint doi: https://doi.org/10.1101/661975; this version posted June 6, 2019. The copyright holder for this preprint (which was not certified by peer review) is the author/funder, who has granted bioRxiv a license to display the preprint in perpetuity. It is made available under aCC-BY-ND 4.0 International license.

Figure 3: Modeling of neurite retraction.

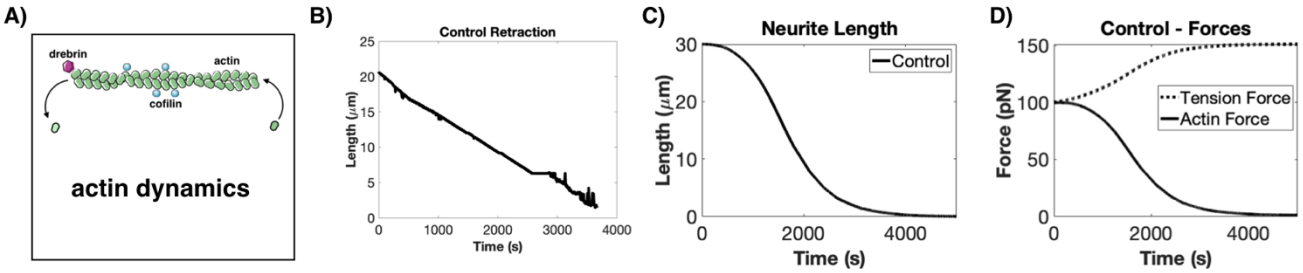

E)

Retraction Start Times of Control Cells	
Neurite 1	2.2 minutes
Neurite 2	2.4 minutes
Neurite 3	8.0 minutes
Neurite 4	7.8 minutes
Neurite 5	2.6 minutes
Neurite 6	4.0 minutes
Neurite 7	4.2 minutes
Neurite 8	2.5 minutes

A) Simplified schematic of actin dynamics depicting assembly/disassembly as a combination of effects due to actin, cofilin, and drebrin concentration**. B)** Example of the retraction in response to carbachol stimulation of differentiated PC12 cells transfected with mCherry-actin. Identical behavior was seen over an average of 8 neurites shown in the table **E). C)** Computational results for neurite retraction determined from the described model. **D)** Calculation of force plots due to increased tension in response to PI(4,5)P_2 hydrolysis, internalization of ligand-bound GPCRs, and tension effects. The force due to actin decreases and switches direction in response to actin breakdown and retrograde flow. **E)** Table showing the variation of retraction times within the same condition**.**

bioRxiv preprint doi: https://doi.org/10.1101/661975; this version posted June 6, 2019. The copyright holder for this preprint (which was not certified by peer review) is the author/funder, who has granted bioRxiv a license to display the preprint in perpetuity. It is made available under aCC-BY-ND 4.0 International license.

Figure 4: Experimental validation of model predictions

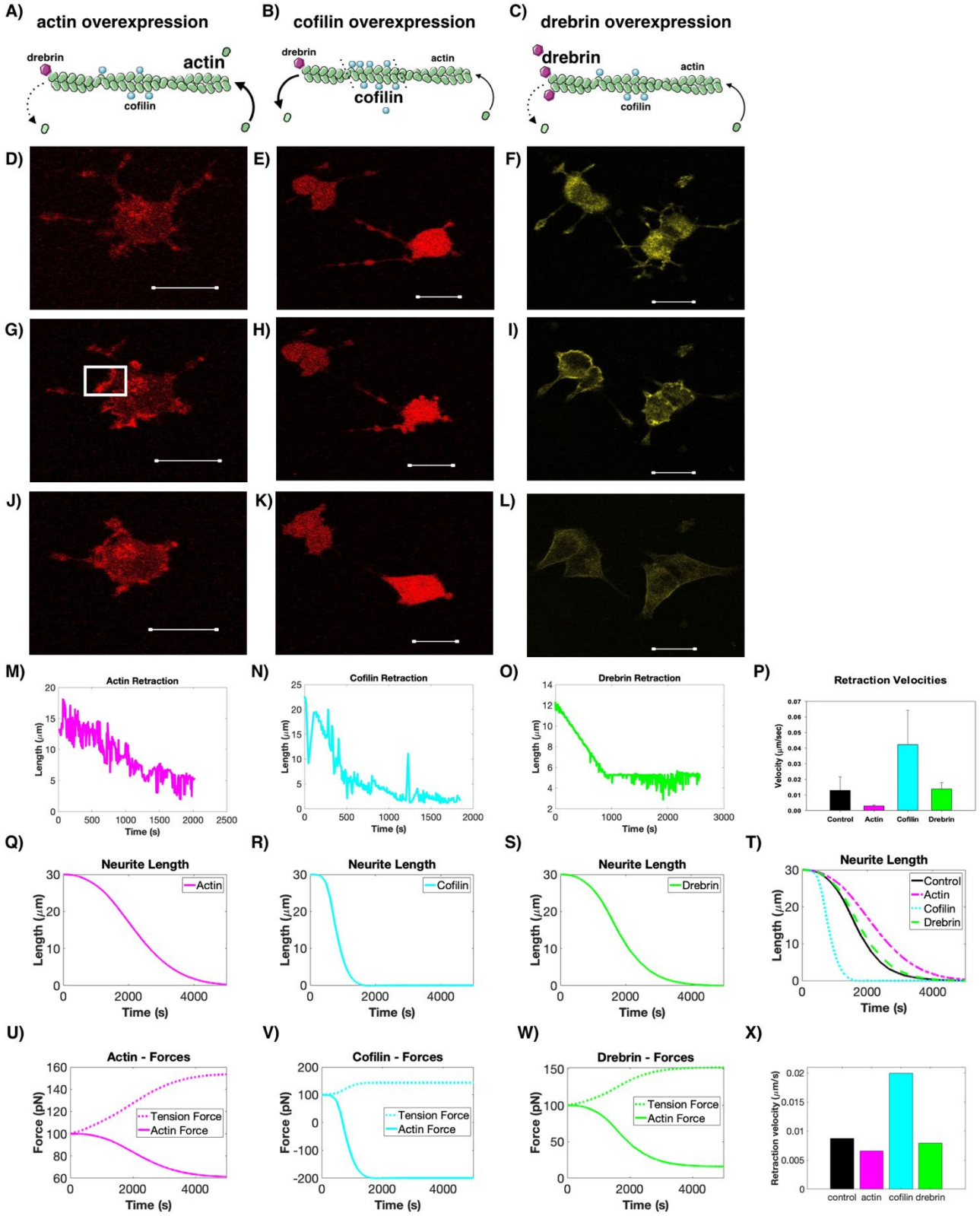

bioRxiv preprint doi: https://doi.org/10.1101/661975; this version posted June 6, 2019. The copyright holder for this preprint (which was not certified by peer review) is the author/funder, who has granted bioRxiv a license to display the preprint in perpetuity. It is made available under aCC-BY-ND 4.0 International license.

Figure 4: **A-C)** Schematic of the experimental study to test the actin force model where mCherry-actin, mCherry-cofilin or eYFP-Drebrin was expressed at varying levels in PC12 cells using increasing amounts of DNA in the transfections. The corresponding images shown directly below. While cofilin activity is mediated by calcium, actin and drebrin dynamics depend on local concentrations.

Column 1 (panels **A, D, G, J, M, Q, U**) are results from studies following mCherry-actin expressed in PC12 cells. The increase in actin, as estimated by western blotting, reduces the change in the actin force. Panel **D** is an example image of cells before carbachol stimulation. **G** is 15 minutes post-stimulation showing the beginning stage of actin breakdown indicated by the white box, and **J** is 30 minutes post-stimulation. A representative retraction velocity curve is shown in **M**. Panels **Q** and **U** are the results of modeling the retraction velocity **(Q)**, due to a tension force and actin force (**U**). We note that the overexpression of actin leads to less of a decrease in actin force since the increased actin concentration slows overall actin breakdown.

Column 2 (panels **B, E, H, K, N, R, V**) shows how cofilin overexpression creates a large negative actin force to increase the rate of disassembly as shown in the schematic **(B)**. Panel **E** is an example image of cells expressing cofilin-RFP before carbachol stimulation, **H** is 7 minutes post-stimulation, and **K** is 16 minutes post-stimulation. A representative retraction velocity curve is shown in **N**. Panel **R** and **V** are the results of modeling the retraction velocity **(R)**, due to the tension force and a larger negative actin force (**V**), since increased cofilin concentration increases actin breakdown.

Column 3 (panels **C, F, I, L, O, S, W**) shows how drebrin overexpression slows the change in actin force as shown in the schematic **(C)**. Panel **F** is an example image of cells expressing drebrin-eYFP before carbachol stimulation. **I** is 15 minutes post-stimulation, and **L** is 30 minutes post-stimulation. A representative retraction velocity curve is shown in **O**. A representative retraction velocity curve is shown in **O**. Panels **S** and **W** are the results of modeling the retraction velocity **(S)**, due to the tension force and actin force (**W**). We note that increased drebrin concentration resists actin breakdown.

Panels **P**, **T** and **X** are compiled retraction velocities obtained experimentally **(P)**, control (n=4), actin(n=4), cofilin(n=3), drebrin(n=4) showing standard error, and computationally (**T** and **X**), showing the very close correlation between experimental and theoretical results. All scale bars = 20 μm.

bioRxiv preprint doi: https://doi.org/10.1101/661975; this version posted June 6, 2019. The copyright holder for this preprint (which was not certified by peer review) is the author/funder, who has granted bioRxiv a license to display the preprint in perpetuity. It is made available under aCC-BY-ND 4.0 International license.

Figure 5: Neurite retraction can be induced by membrane tension in response to hyper-osmotic stress.

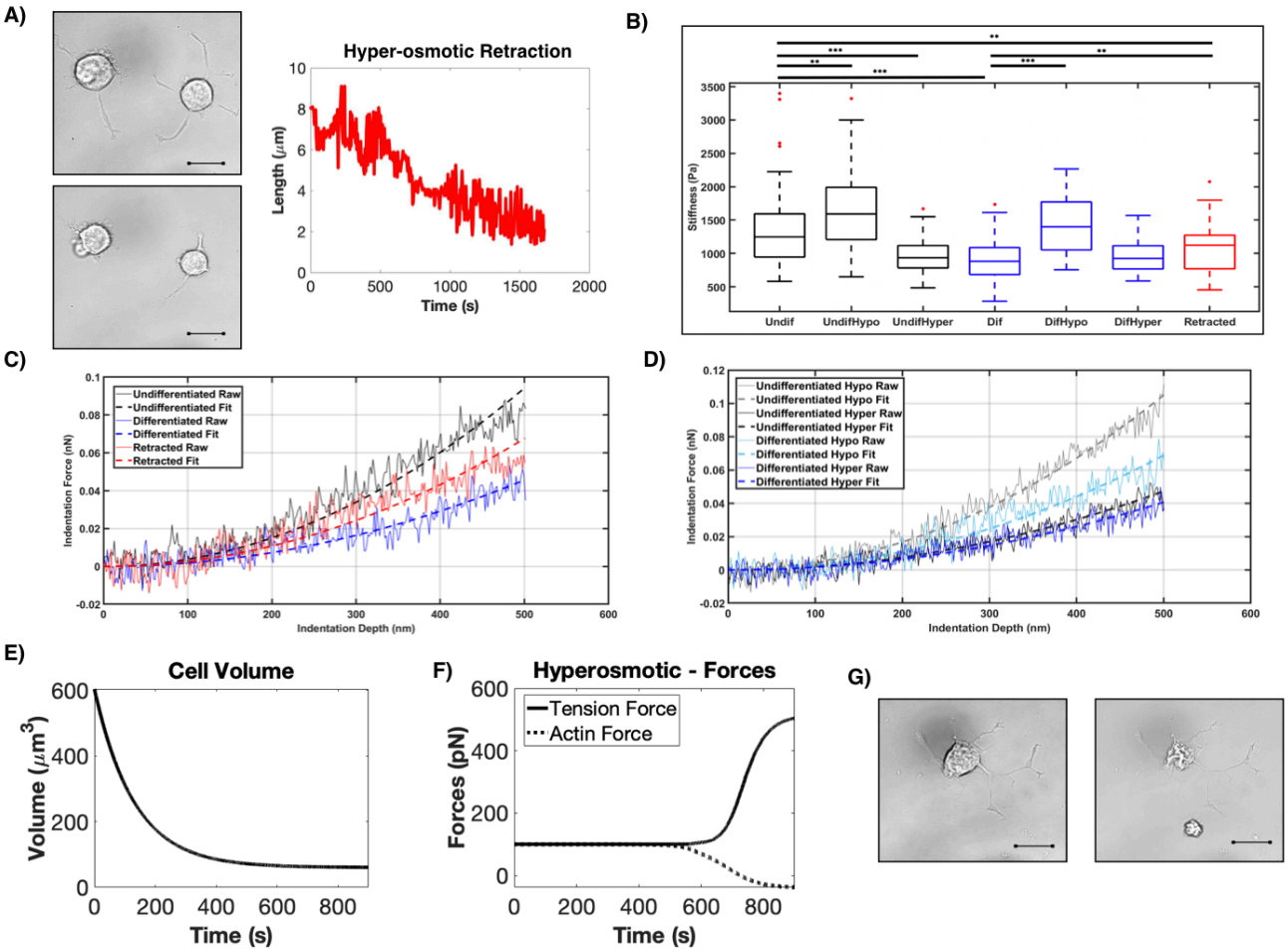

A) Phase contrast images of PC12 cells under isotonic conditions (300 mOsm, *top left*) and hyper-osmotic conditions (450 mOsm, *bottom left*) after 10 minutes). The corresponding neurite retraction curve for the cell on the left is shown to the right. **B)** Cell stiffness as measured by atomic force microscopy of undifferentiated and differentiated PC12 cells under isotonic conditions and cells subjected to hypo-osmotic (150 mOsm) or hyper-osmotic (450 mOsm) stress where the number of cells n =14 – 46, and were * = $p < 0.05$, ** = $p < 0.01$, ***= $p < 0.001$. **C-D)** Force curves representative of the average stiffness values in B with automated Hertz model fitting *(see methods)* over 500nm indentation for untreated cells (*left*) and hypo-osmotic /hyper-osmotic treated cells (*right*). **E-F)** Hyperosmotic stress is modeled as an instantaneous increase in membrane tension due to the reduction in volume-to-surface area ratio, which causes a membrane tension increase and a smaller cytoskeletal force (E), and triggers neurite retraction (F) in the absence of ligand input. **G)** Phase contrast images of a differentiated PC12 cells before the application of osmotic stress (*left*) and after increasing the osmolarity from 300 to 600 mOsm in calcium-free media. Note the loss in cell volume seen by membrane puckering but without retraction (*right*)

bioRxiv preprint doi: https://doi.org/10.1101/661975; this version posted June 6, 2019. The copyright holder for this preprint (which was not certified by peer review) is the author/funder, who has granted bioRxiv a license to display the preprint in perpetuity. It is made available under aCC-BY-ND 4.0 International license.

Figure 6: Neurite retraction induced by membrane tension is seen in the neural network of *C.elegans*

A)

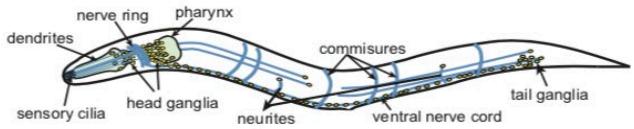

B)

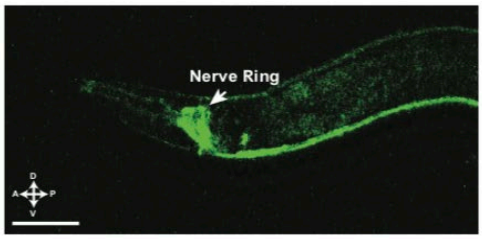

C)

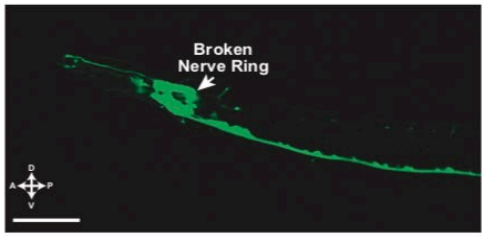

D)

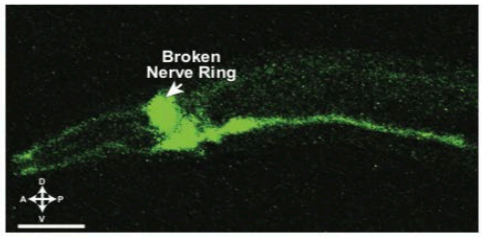

E)

Treatment	Nr. of worms	% worms showing neurite retraction
Control	3	0%
Carbachol	10	100%
NaCl	6	100%

F)

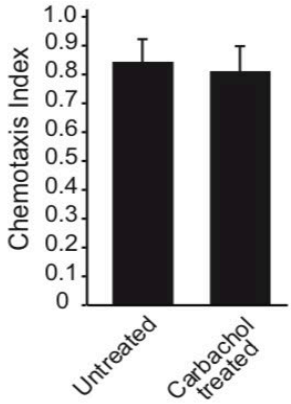

A) General schematic of the nervous system of C. *elegans.* **B**) Untreated C. *elegans* that expresses GFP G-CAMP through the nerve ring and ventral nerve. **C**) A representative worm with 1mM carbachol for 30 minutes showing a broken nerve ring and pilling ventral nerve. **D**) A representative worm subjected to hyper-osmotic stress showing a broken nerve ring. **E**) Table showing the compiled results of each experimental condition and the number of resulting nerve rings that were broken. **F**) Results of a chemotaxis assay testing movement of C. *elegans* with and without lmM carbachol treatment.

bioRxiv preprint doi: https://doi.org/10.1101/661975; this version posted June 6, 2019. The copyright holder for this preprint (which was not certified by peer review) is the author/funder, who has granted bioRxiv a license to display the preprint in perpetuity. It is made available under aCC-BY-ND 4.0 International license.

REFERENCES

Berstein, G., Blank, J.L., Jhon, D.-Y., Exton, J.H., Rhee, S.G., and Ross, E.M. (1992). Phospholipase C-β1 is a GTPase-Activating Protein for $G_{q/11}$, Its Physiologic Regulator. Cell *70*, 411-418.

Bittner, M.A., and Holz, R.W. (2005). Phosphatidylinositol-4,5-bisphosphate: actin dynamics and the regulation of ATP-dependent and -independent secretion. Mol Pharmacol *67*, 1089-1098.

Bornschlogl, T., Romero, S., Vestergaard, C.L., Joanny, J.F., Van Nhieu, G.T., and Bassereau, P. (2013). Filopodial retraction force is generated by cortical actin dynamics and controlled by reversible tethering at the tip. Proc Natl Acad Sci U S A *110*, 18928-18933.

Brini, M., Cali, T., Ottolini, D., and Carafoli, E. (2014). Neuronal calcium signaling: function and dysfunction. Cellular and molecular life sciences : CMLS *71*, 2787-2814.

Calabrese, B., Saffin, J.M., and Halpain, S. (2014). Activity-dependent dendritic spine shrinkage and growth involve downregulation of cofilin via distinct mechanisms. PLoS One *9*, e94787.

Clapham, D.E. (2007). Calcium Signaling. Cell *131*, 1047-1058.

Datar, A., Ameeramja, J., Bhat, A., Srivastava, R., Bernal, R., Prost, J., Callan-Jones, A., and Pullarkat, P.A. (2019). The roles of microtubules and membrane tension in axonal beading, retraction, and atrophy. bioRxiv, 575258.

Diz-Munoz, A., Fletcher, D.A., and Weiner, O.D. (2013). Use the force: membrane tension as an organizer of cell shape and motility. Trends Cell Biol *23*, 47-53.

Dohlman, H.G., and Thorner, J. (1997). RGS Proteins and Signaling by Heterotrimeric G Proteins. The Journal of Biological Chemistry *272*, 3871-3874.

Drubin, D.G., Feinstein, S.C., Shooter, E.M., and Kirschner, M.W. (1985). Nerve growth factor-induced neurite outgrowth in PC12 cells involves the coordinate induction of microtubule assembly and assembly-promoting factors. The Journal of Cell Biology *101*, 1799-1807.

Franze, K., Gerdelmann, J., Weick, M., Betz, T., Pawlizak, S., Lakadamyali, M., Bayer, J., Rillich, K., Gogler, M., Lu, Y.B.*, et al.* (2009). Neurite branch retraction is caused by a threshold-dependent mechanical impact. Biophys J *97*, 1883-1890.

Freedman, N.J., and Lefkowitz, R.J. (1996). Desensitization of G protein-coupled receptors. Recent Progress in Hormone Research *51*, 319-351; discussion 352-313.

Garcia, P., Gupta, R., Shah, S., Morris, A.J., Rudge, S.A., Scarlata, S., Petrova, V., McLaughlin, S., and Rebecchi, M.J. (1995). The pleckstrin homology domain of phospholipase C-delta 1 binds with high affinity to phosphatidylinositol 4,5-bisphosphate in bilayer membranes. Biochemistry *34*, 16228-16234.

Getz, M., Swanson, L., Sahoo, D., Ghosh, P., and Rangamani, P. (2019). A predictive computational model reveals that GIV/Girdin serves as a tunable valve for EGFR-stimulated Cyclic AMP Signals. Mol Biol Cell, mbcE18100630.

Gilbert, J., and Man, H.-Y. (2017). Fundamental Elements in Autism: From Neurogenesis and Neurite Growth to Synaptic Plasticity. Front Cell Neurosci *11*, 359-359.

Greene, L.A., and Tischler, A.S. (1976). Establishment of a noradrenergic clonal line of rat adrenal

bioRxiv preprint doi: https://doi.org/10.1101/661975; this version posted June 6, 2019. The copyright holder for this preprint (which was not certified by peer review) is the author/funder, who has granted bioRxiv a license to display the preprint in perpetuity. It is made available under aCC-BY-ND 4.0 International license.

pheochromocytoma cells which respond to nerve growth factor. Proceedings of the National Academy of Sciences of the United States of America *73*, 2424-2428.

Grintsevich, E.E., and Reisler, E. (2014). Drebrin inhibits cofilin-induced severing of F-actin. Cytoskeleton (Hoboken) *71*, 472-483.

Guo, Y., Rebecchi, M., and Scarlata, S. (2005). Phospholipase Cbeta2 binds to and inhibits phospholipase Cdelta1. J Biol Chem *280*, 1438-1447.

Hartzell, C.A., Jankowska, K.I., Burkhardt, J.K., and Lewis, R.S. (2016). Calcium influx through CRAC channels controls actin organization and dynamics at the immune synapse. Elife *5*.

Hassinger, J.E., Oster, G., Drubin, D.G., and Rangamani, P. (2017). Design principles for robust vesiculation in clathrin-mediated endocytosis. Proceedings of the National Academy of Sciences *114*, E1118-E1127.

He, L., Tao, J., Maity, D., Si, F., Wu, Y., Wu, T., Prasath, V., Wirtz, D., and Sun, S.X. (2018). Role of membrane-tension gated Ca(2+) flux in cell mechanosensation. J Cell Sci *131*.

Kadamur, G., and Ross, E.M. (2013). Mammalian Phospholipase C. Annual Review of Physiology *75*, 127-154.

Kerstein, P.C., Nichol, R.I., and Gomez, T.M. (2015). Mechanochemical regulation of growth cone motility. Front Cell Neurosci *9*, 244.

King, A.E., Woodhouse, A., Kirkcaldie, M.T., and Vickers, J.C. (2016). Excitotoxicity in ALS: Overstimulation, or overreaction? Experimental neurology *275 Pt 1*, 162-171.

LaFerla, F.M. (2002). Calcium dyshomeostasis and intracellular signalling in Alzheimer's disease. Nat Rev Neurosci *3*, 862-872.

Licht, T., Goshen, I., Avital, A., Kreisel, T., Zubedat, S., Eavri, R., Segal, M., Yirmiya, R., and Keshet, E. (2011). Reversible modulations of neuronal plasticity by VEGF. Proc Natl Acad Sci U S A *108*, 5081-5086.

Logan, M.R., and Mandato, C.A. (2006). Regulation of the actin cytoskeleton by PIP2 in cytokinesis. Biol Cell *98*, 377-388.

Lohmann, C., and Wong, R.O. (2005). Regulation of dendritic growth and plasticity by local and global calcium dynamics. Cell Calcium *37*, 403-409.

Mattson, M.P. (2007). Calcium and neurodegeneration. Aging Cell *6*, 337-350.

McCullough, B.R., Blanchoin, L., Martiel, J.L., and De la Cruz, E.M. (2008). Cofilin increases the bending flexibility of actin filaments: implications for severing and cell mechanics. J Mol Biol *381*, 550-558.

McKay, S.E., Purcell, A.L., and Carew, T.J. (1999). Regulation of Synaptic Function by Neurotrophic Factors in Vertebrates and Invertebrates: Implications for Development and Learning. Learning & Memory *6*, 193-215.

Mikati, M.A., Grintsevich, E.E., and Reisler, E. (2013). Drebrin-induced stabilization of actin filaments. J Biol Chem *288*, 19926-19938.

Mutalik, S.P., Joseph, J., Pullarkat, P.A., and Ghose, A. (2018). Cytoskeletal Mechanisms of Axonal Contractility. Biophys J *115*, 713-724.

bioRxiv preprint doi: https://doi.org/10.1101/661975; this version posted June 6, 2019. The copyright holder for this preprint (which was not certified by peer review) is the author/funder, who has granted bioRxiv a license to display the preprint in perpetuity. It is made available under aCC-BY-ND 4.0 International license.

Nair, R.R., Patil, S., Tiron, A., Kanhema, T., Panja, D., Schiro, L., Parobczak, K., Wilczynski, G., and Bramham, C.R. (2017). Dynamic Arc SUMOylation and Selective Interaction with F-Actin-Binding Protein Drebrin A in LTP Consolidation In Vivo. Front Synaptic Neurosci *9*, 8.

Nourse, J.L., and Pathak, M.M. (2017). How cells channel their stress: Interplay between Piezo1 and the cytoskeleton. Semin Cell Dev Biol *71*, 3-12.

Pavlov, D., Muhlrad, A., Cooper, J., Wear, M., and Reisler, E. (2007). Actin filament severing by cofilin. J Mol Biol *365*, 1350-1358.

Rangamani, P., Fardin, M.A., Xiong, Y., Lipshtat, A., Rossier, O., Sheetz, M.P., and Iyengar, R. (2011). Signaling network triggers and membrane physical properties control the actin cytoskeleton-driven isotropic phase of cell spreading. Biophys J *100*, 845-857.

Raucher, D., Stauffer, T., Chen, W., Shen, K., Guo, S., York, J.D., Sheetz, M.P., and Meyer, T. (2000). Phosphatidylinositol 4,5-bisphosphate functions as a second messenger that regulates cytoskeleton-plasma membrane adhesion. Cell *100*, 221-228.

Rosenberg, S.S., and Spitzer, N.C. (2011). Calcium signaling in neuronal development. Cold Spring Harb Perspect Biol *3*, a004259.

Sharma, S., Grintsevich, E.E., Phillips, M.L., Reisler, E., and Gimzewski, J.K. (2011). Atomic force microscopy reveals drebrin induced remodeling of f-actin with subnanometer resolution. Nano Lett *11*, 825-827.

Sheetz, M.P. (2001). Cell control by membrane-cytoskeleton adhesion. Nat Rev Mol Cell Biol *2*, 392-396.

Sheetz, M.P., and Dai, J. (1996). Modulation of membrane dynamics and cell motility by membrane tension. Trends Cell Biol *6*, 85-89.

Simunovic, M., Manneville, J.B., Renard, H.F., Evergren, E., Raghunathan, K., Bhatia, D., Kenworthy, A.K., Voth, G.A., Prost, J., McMahon, H.T.*, et al.* (2017). Friction Mediates Scission of Tubular Membranes Scaffolded by BAR Proteins. Cell *170*, 172-184 e111.

Stuchlik, A. (2014). Dynamic learning and memory, synaptic plasticity and neurogenesis: an update. Front Behav Neurosci *8*, 106-106.

Takeuchi, T., Duszkiewicz, A.J., and Morris, R.G.M. The synaptic plasticity and memory hypothesis: encoding, storage and persistence. Philos Trans R Soc Lond B Biol Sci *369*, 20130288-20130288.

van Rheenen, J., and Jalink, K. (2002). Agonist-induced PIP(2) hydrolysis inhibits cortical actin dynamics: regulation at a global but not at a micrometer scale. Mol Biol Cell *13*, 3257-3267.

Voglis, G., and Tavernarakis, N. (2006). The role of synaptic ion channels in synaptic plasticity. EMBO Rep *7*, 1104-1110.

West, A.E., Chen, W.G., Dalva, M.B., Dolmetsch, R.E., Kornhauser, J.M., Shaywitz, A.J., Takasu, M.A., Tao, X., and Greenberg, M.E. (2001). Calcium regulation of neuronal gene expression. Proceedings of the National Academy of Sciences *98*, 11024-11031.

Zmurchok, C., Bhaskar, D., and Edelstein-Keshet, L. (2018). Coupling mechanical tension and GTPase signaling to generate cell and tissue dynamics. Phys Biol *15*, 046004.